Biosensors and Bioelectronics 142 (2019) 111544

Contents lists available at ScienceDirect

Biosensors and Bioelectronics

journal homepage: www.elsevier.com/locate/bios

Double signal amplification strategy for ultrasensitive electrochemical biosensor based on nuclease and quantum dot-DNA nanocomposites in the detection of breast cancer 1 gene mutation

Bin Yang, Song Zhang*, Xueen Fang, Jilie Kong**

Department of Chemistry and Institutes of Biomedical Sciences, Fudan University, Shanghai, 200438, PR China

ARTICLE INFO

Keywords:
Cyclic enzymatic signal amplification
DNA nanotechnology
Double signal amplification
Electrochemical DNA biosensor
BRCA1
microRNA

ABSTRACT

Rapid and efficient detection of microRNA (miRNA) of breast cancer 1 gene mutation (BRCA1) at their earliest stages is one of the crucial challenges in cancer diagnostics. In this study, a highly-sensitive electrochemical DNA biosensor was fabricated by double signal amplification (DSA) strategy for the detection of ultra-trace miRNA of BRCA1. In the presence of target miRNA of BRCA1, the well-matched RNA-DNA duplexes were specifically recognized by double-strand specific nuclease (DSN), and the DNA part of the duplexes were then cleaved and miRNAs were released to trigger another following cycle, which produced a primarily amplified signal by such a cyclic enzymatic signal amplification (CESA). Then triple-CdTe quantum dot labelled DNA nanocomposites (3-QD@DNA NC) was selectively hybridized with the cleaved DNA probe on the electrode and produced multiply amplified signals. The biosensor exhibited a high sensitivity for the detection of miRNA of BRCA1 in concentrations ranging from 5 aM to 5 fM, and its detection limit of 1.2 aM was obtained, which is two or three orders of magnitude lower than those by single signal amplification strategy such as CESA or QD-labeled DNA probes. The as-prepared biosensor was successfully used to detect the miRNA of BRCA1 in human serum samples with acceptable stability, good reproducibility, and good recovery. The proposed DNA biosensor based on double signal amplification strategy provided a feasible, rapid, and sensitive platform for early clinical diagnosis and practical applications.

1. Introduction

Breast cancer is a major leading cause of cancer death among women across the world, especially in the United States, which approximately accounts for one third of all the cancer cases (Siegel et al., 2019; Umetani et al., 2006; Snell et al., 2008; Zhao et al., 2017). Moreover, breast cancer as one of the metastatic cancer still is an incurable disease. The early-diagnosis for breast cancer plays an essential role in reducing the morbidity and mortality, and avoiding long-term ineffective treatments and side-effects (Beenken and Mohammadi, 2009; Jackson and Bartek, 2009; Wilson and Hay, 2011). Although the diagnostic techniques of breast cancer have greatly improved in recently years, the lack of specific biomarkers still limits the early diagnosis of breast cancer (Fan et al., 2018). Notably, the low-level promoter mutation of breast cancer 1 (BRCA1) in human peripheral blood or normal tissues resulted in some post-transcriptional regulators, such as miRNA, a class of small-sequence noncoding RNA (typically 18–25 nucleotides) (Chan et al., 2013; Ng et al., 2013). The miRNA can be used as a potential diagnostic biomarker of BRCA1, which has been reported that plays a critical role in prevention and therapy-target treatment of breast cancer (Mendell, 2016; Fish et al., 2018; Tavazoie et al., 2008). For this regard, some methods for the detection of circulating miRNA were developed, i.e. northern blotting (Rooij et al., 2006), microarrays (Li and Ruan, 2009), real-time polymerase chain reaction (RT-PCR) (Asaga et al., 2011; Cuk et al., 2013; Schrauder et al., 2012), rolling circle amplification (RCA) (Fan et al., 2018), miRNA next-generation sequencing (Wu et al., 2011; Volinia et al., 2012), real-time fluorescence microfluidics (Mavrogiannopoulou et al., 2009), and quadratic isothermal amplification (Duan et al., 2013). Compared with these analytical strategies, the development of biosensors attracted more attention in the detection of miRNA of BRCA1 gene mutation because of the advantages, such as high sensitivity, high selectivity, low cost, and easy operation (Rasheed and Sandhyarani, 2015; Chen et al., 2017; Cui et al., 2017; Li et al., 2012; Yang et al., 2016). Due to low-

* Corresponding author.
** Corresponding author.
E-mail addresses: songzhang@fudan.edu.cn (S. Zhang), jlkong@fudan.edu.cn (J. Kong).

https://doi.org/10.1016/j.bios.2019.111544
Received 28 May 2019; Received in revised form 20 July 2019; Accepted 26 July 2019
Available online 27 July 2019
0956-5663/

abundance and degradation susceptibility of miRNA of BRCA1, it is important to develop an ultrasensitive biosensor with an effective signal amplification in order to realize the early diagnosis for breast cancer.

The advances of nanotechnology by combining DNA with nanomaterials provides a new strategy of signal amplification for the biosensors in early diagnosis. The DNA nanotechnology can not only use DNA rigid strands to construct highly-ordered structure at the nanoscale programmably, but also utilize the controllable and pre-designed DNA manner to bind with nanomaterials, such as quantum dots (QDs), to produce stable and amplified signal (Liu et al., 2017; Seeman, 2003; Vittala et al., 2017; Su et al., 2014; Zhang et al., 2016; Wang et al., 2018). Some DNA molecular probes, including QDs/Y-shaped DNA nanosphere (Wen et al., 2018) and Au nanoparticle/bridge DNA structure (Bo et al., 2018), were devised to produce signal amplification in bioanalysis. A decomposable QDs/DNA nanosphere probe was fabricated to detect extracellular respiring bacteria by conjugating multiple QDs with Y-shaped DNA, and being decomposed to release a great number of QDs with a detection limit of 1.37 cfu/mL (Wen et al., 2018). Compared with single-labelled probes, where a probe with a reporter molecule, multiple-labelled DNA probes have better analytical performance in signal amplification. However, even for the QD-DNA nanocomposite, the limit of detection will be normally restricted within the pM-to-nM range because of the detection relies only on the hybridization events of DNA (Wang et al., 2018), which are not enough to detect ultra-trace miRNAs for early patients of breast cancer. Other effective amplification strategy in miRNA detection is combining the isothermal amplification methods with the QD-based nanosensors, such as exponential amplification reaction (Fan et al., 2018), catalytic hairpin assembly amplification (Li et al., 2015), target-recycled enzyme-free amplification (Loo et al., 2016) and enzymatic amplification (Xu et al., 2012). Double enzyme amplification based on isothermal amplification and exonuclease cycle reaction via a designed functional molecular beacon with highly specific sequence (Duan et al., 2013), and this approach with a detection limit of 10 fM was highly sensitive for the detection of miRNA of breast cancer.

In previous work, we developed two ultrasensitive aptasensors for the detection of low quantity cancer cells by combining cyclic enzymatic signal amplification (CESA) with gold nanoparticles (Zhang et al., 2014) and graphene oxide (GO) (Xiao et al., 2017), respectively, and the limit of detections attained 40 and 25 cells. Some electrochemical aptasensors with high sensitivity were developed by combining exonuclease III-assisted cyclic amplification with a nanoporous gold microelectrode for the detection of bisphenol A and ochratoxin A (Shi et al., 2018), or with vertical single-walled carbon nanotubes (Shi et al., 2017a) and 3D graphene/gold film (Shi et al., 2017b) for the detection of mercury. Notably, in order to detect ultra-trace miRNA in peripheral blood, it is necessary to improve the sensitivity of aptasensors by the combination of CESA and DNA-modified nanomaterials. In this study, double signal amplification (DSA) strategy for the ultrasensitive detection of miRNA was developed based on CESA with a double-strand specific nuclease (DSN) and triple QD-DNA nanocomposites (3-QD@DNA NC) as a cascade signal probe (shown as Fig. 1). Herein, CESA was firstly conducted to ultra-specifically recognize the target miRNA of BRCA1, because DSN showed a satisfactory ability to discriminate between well-matched and mismatched short duplex DNA (up to one mismatched base), and the DNA of the RNA-DNA duplex were cleaved selectively and the free miRNA were released to trigger another cycle (Yin et al., 2012; Zhao et al., 2007). The as-prepared 3-QD@DNA NC was then introduced into the system by the in-situ hybridization on the biosensor, giving a multiply-enhanced current signal. Notably, compared with those biosensors with single amplification strategy such as QD-DNA (You et al., 2018) and CESA (Cui et al., 2017), the electrochemical biosensor based on DSA strategy would have higher sensitivity and excellent selectivity, which would be benefit to the detection of ultra-trace target miRNA of BRCA 1 in peripheral blood samples and the early diagnosis for breast cancer.

2. Materials and methods

2.1. Apparatus and materials

The information on Apparatus and Materials including all the oligonucleotides sequences used in this study is shown in Supporting Information.

2.2. Preparation of 3-QD@DNA NC and a QD@DNA NC

The water-soluble CdTe QDs modified with mercaptoacetic acid (TGA) was prepared and purified according to the previous report (Amin et al., 2017), and stored in 4 °C when not used. Then, CdTe QDs-TGA were further linked with NH_2 labeled single stranded DNA (ssDNA) 1 and 2 through EDC/NHS coupling. Briefly, two NH_2 functionalized ssDNA (1 and 2) with the ratio of 2:1 were dissolved in Tris-HCl buffer (pH 7.4, 25 °C), and then 1 mL of as-prepared CdTe QDs-TGA solution was added into the ssDNA1/ssDNA2 mixture solution (0.25 mg/mL EDC, 0.25 mg/mL NHS) in 37 °C for 16 h. After that, the functionalized DNA were purified by eliminating excess reagents by centrifugation of 12,000 rpm for 1 min. The precipitate was dispersed in 1 mL of PBS buffer (pH 7.4, 25 °C).

3-QD@DNA NC was prepared by the hybridization of single-stranded DNA 1 and 2 (Amin et al., 2017). Briefly, 12 μmol/L bridge DNA 1 and 2 solutions were mixed with equal volume and incubated in 95 °C for 2 min. After being cooled down (25 °C), the obtained DNA structure was mixed with the QDs functionalized ssDNA for 3-h hybridization. Finally, the obtained 3-QD@DNA NC was purified via centrifugation at 12,000 rpm for 1 min and dispersed in 1 mL PBS buffer (pH 7.4).

And a QD@DNA NC was prepared by CdTe QDs single label method. 12 μmol/L bridge DNA 2 solution was incubated in 95 °C for 2 min. After being cooled down (25 °C), the obtained DNA structure was mixed with the QDs functionalized ssDNA 1 for 3-h hybridization. Finally, the obtained a QD@DNA NC was purified via centrifugation at 12,000 rpm for 1 min and dispersed in 1 mL PBS buffer (pH 7.4).

2.3. DNA biosensor construction

The surface of the gold electrode was polished with finer-grade aqueous alumina slurries (1.0, 0.3 and 0.05 μm grain sizes) successively on a chamois leather, followed by alternately washing with ethanol-HNO_3 (V:V, 1:1) and double-distilled water.

The bare gold electrode (GE) was dipped into 40 μL 0.01 M TE buffer (pH 8.0) including 10 μL 10 μM of capture DNA (cDNA) under 37 °C. Then the electrode was transferred into 1 mM MCH solution for 1 h under 37 °C in order to decrease background signal and nonspecific adsorption. After that, the electrode was washed with TE buffer (0.01 M, pH 8.0) and double-distilled water. The modified electrode was incubated in 0.05 M Tris-HCl buffer (pH 8.0) with different concentrations of miRNA target and 0.1 U DSN, 5 mM $MgCl_2$, 1 mM DTT for 50 min under 37 °C. After washing with TE buffer (0.01 M, pH 8.0) as well as double-distilled water, the electrode was put in as-prepared 3-QD@DNA NC for hybridization (40 min, 50 °C). Finally, the electrode was washed as mentioned above and then transferred to electrochemical platform for miRNA of BRCA1 determination.

2.4. Electrochemical measurements

Differential pulse voltammetry (DPV) testing was conducted for BRCA1 determination. The scanning potential range was set from 0 V to 0.5 V at a scan rate of 100 mV/s in a 0.02 mol/L Tris-HCl buffer solution (pH 7.5, 25 °C).

Cyclic voltammetry (CV) measurement was conducted for electrochemical characterization. The scanning potential range was set from −0.2 V to 0.6 V at a scan rate of 100 mV/s in a 0.05 mol/L K_3[Fe

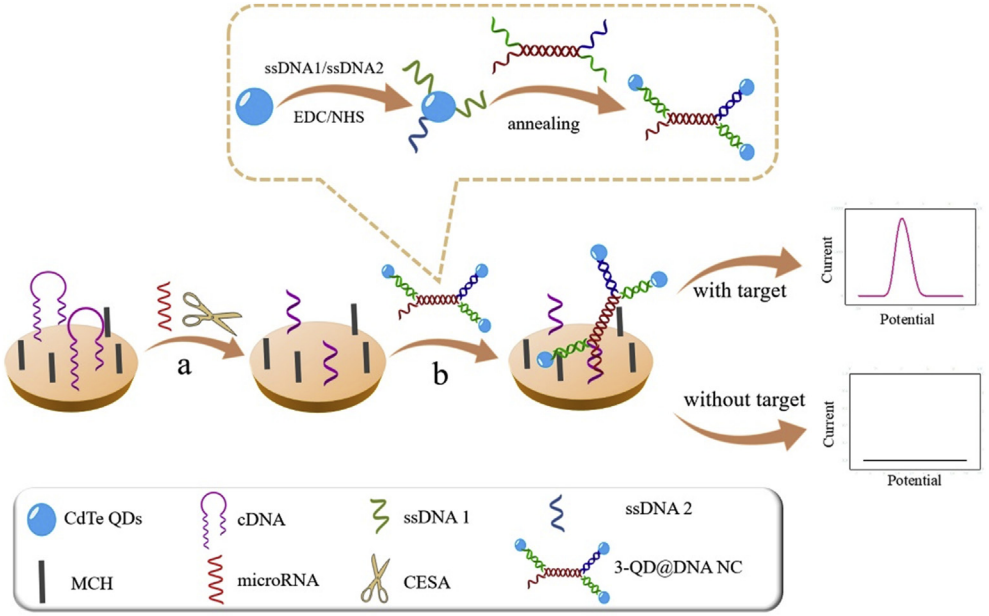

Fig. 1. Schematic diagrams of the ultrasensitive DNA biosensor for the detection of miRNA. The DSA strategy had a) a CESA process with DSN and miRNA, and b) a hybridization with the probe of 3-QD@DNA NC.

$(CN)_6]/K_4[Fe(CN)_6]$ solution that contained 0.50 mol/L KCl. Electrochemical impedance spectroscopy (EIS) was performed in the frequency range of 0.1 Hz–100,000 Hz and at an alternating voltage of 5 mV. All the electrochemical measurements were performed at room temperature (25 °C).

2.5. Sample treatment

Healthy human serum samples were supplied by school hospital of Fudan University. All the samples were followed by centrifugation at 1500 rpm/min for 20 min to eliminate sediment as well as insoluble substance, and diluted by 10 times. Trizol kit was employed to extract RNA from the samples.

3. Results and discussion

3.1. Principle of the electrochemical biosensor for the miRNA of BRCA1 ultrasensitive detection with DSA strategy

The principle of DSA strategy of this biosensor for the ultrasensitive detection of BRCA1 was shown as Fig. 1. The specific binding of cDNA to target miRNA triggered a CESA process, and then detected by a hybridization with the signal probe of 3-QD@DNA NC. The quantitative detection of miRNA was realized by such DSA strategy. Herein, the cDNA/GE was firstly fabricated by a self-assemble process with cDNA to capture target miRNA, and MCH to avoid nonspecific nucleic acid absorption and then decrease the background signal. When incubated with miRNA and DSN, the CESA reaction was triggered with the special binding of cDNA and miRNA, and the DNA part of the well-matched duplex was cleaved selectively and the free miRNA was released to trigger another cycle. The 3-QD@DNA NC was hybridized with the cleaved cDNA/GE to produce an enhanced DPV current signal. Whereas there was no miRNA, the cDNA/GE was just incubated with DSN and 3-QD@DNA NC and would not show a DPV signal. The sensitivity of this method would be greatly improved by DSA with CESA and 3-QD@DNA NC. Moreover, the selectivity of the method would be improved because DSN could only digest the DNA of the perfectly matched RNA-DNA duplex, instead of the imperfectly matched one.

3.2. Characterization of the signal probe 3-QD@DNA NC

The 3-QD@DNA NC was prepared as the sensitive electrochemical signal probe and characterized by TEM, UV–Vis, infrared (IR) and other spectra. From the TEM, the 3-QD@DNA NC shows a stable microstructure with three CdTe nanoparticles (Fig. 2A), which was accurately manipulated by a special DNA sequence in order to retain a hybrid DNA sequence and multiple electrochemical signals of CdTe QDs. 3-QD@DNA NC was composed of two strand bridge DNA (33 bases). And it could be also seen an obvious visible band around at 50 bp via agarose gel electrophoresis in Supporting Information (Fig. S5), manifesting the successful synthesis the DNA nano-structures. The single QD had a spherical shape with an average size of ~15 nm (Fig. 2B and C). Also, the characterized band at 1384 cm^{-1} of the QDs corresponding to V_s of COO^- could be seen in their Raman spectrum (Fig. 2D), indicating that –COOH group was successfully combined with CdTe QDs (Michota and Bukowska, 2003). The spectra characterizations including UV–Vis, fluorescence, IR, and energy dispersive spectra also confirmed the successful formation of stable CdTe QDs and 3-QD@DNA NC (Supporting Information, Figs. S1–S4). In comparison of single-labeled DNA framework, QDs could be aggregated via spatial conformational DNA strands in 3-QD@DNA NC (multiple QDs-labeled DNA framework), which could be used as a sensitive electrochemical probe.

3.3. Validation of the biosensor based on DSA strategy

To validate the DSA strategy for the ultrasensitive detection of miRNA, the molecular events occurred on the GE was firstly tested by agarose gel electrophoresis (as Fig. 3A). In presence of cDNA, miRNA and DSN, the new band about 50 bp was seen in lane 3, and it was not found in lane 4, which were only presence of cDNA and miRNA. Compared with the pure cDNA (lane 1) and miRNA (lane 2), the new band was ascribed to the cleavage product of CESA. Herein, the special binding of cDNA and miRNA and DSN were necessary conditions for such a CESA. In such a CESA system, the good selectivity and signal amplification could be ascribed to the good efficiency of DSN, which could digest specifically the well-matched dsDNA, and no mismatched short duplex DNA (up to one mismatched base) or ssDNA. Meanwhile the specific binding of cDNA and target miRNA would be amplified many times by the DSN-cleaved reactions (as shown in Fig. 1).

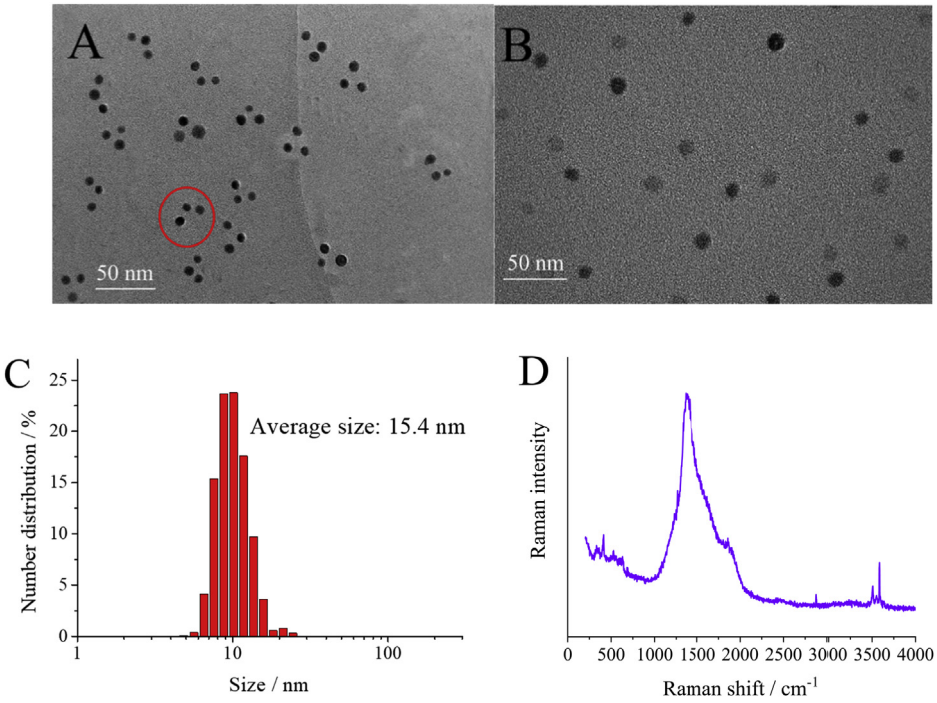

Fig. 2. Characterizations of the signal probe of 3-QD@DNA NC and CdTe QDs. TEM graphs of (A) 3-QD@DNA NC and (B) CdTe QDs. (C) The particle size distribution and (D) Raman spectrum of CdTe QDs.

DPV experiments were also performed to test the DSA strategy for the detection of miRNA. Compared with the blank (Fig. 3B, a), an obvious current response was found for the biosensor with DSN and 3-QD@DNA NC (Fig. 3B, b), which primarily implied the feasibility of the DSA strategy. And the current response (Fig. 3B, b, 1.15 μA) was higher than those in QD@DNA NC with DSN (Fig. 3B, c, 0.34 μA) and 3-QD@DNA NC without DSN (Fig. 3B, d, 0.016 μA). Thus, the biosensor based on DSA strategy achieved an enhancing signal output and a remarkable magnification factor. The detailed current response results were shown in Supporting Information (in Fig. S6). All these results indicated that the special binding of cDNA and miRNA, DSN and 3-QD@DNA NC were necessary for the ultrasensitive detection of miRNA in order to attain multiply signal amplification.

3.4. Characterization of the biosensor

The electrochemical behaviors of the DNA biosensor in the preparation and the detection were investigated by CV in a fairly reversible redox couple of $[Fe(CN)_6]^{3-/4-}$. As shown as Fig. 4A, the decreased current of redox peaks for cDNA/GE (curve b) than that for bare GE (curve a), implies the immobilization of cDNA on the GE by a self-assembled process. While incubated with miRNA and DSN, the increased current of redox peaks for cDNA/GE (curve c) than that for cDNA/GE (curve b) was found, indicating the cDNA on the GE were cleaved by DSN due to the specific binding of cDNA and miRNA (as shown as Fig. 1). Then incubated with 3-QD@DNA NC, the obviously decreased current of redox peaks for cDNA/GE (curve d) than that for cDNA/GE (curve c) was observed, indicating the hybridization of 3-QD@DNA NC with the cleaved cDNA impeded the electron transfer of the redox probes towards GE.

The changes in charge transfer resistance (R_{ct}) of the cDNA/GE biosensor were also investigated by EIS as a sensitive tool to detect the interfacial properties. Fig. 4B showed Nyquist plots of the biosensors measured by EIS. All the plots exhibited a semicircle portion at high frequencies indicating it is a charge-transfer limited process, and a linear portion at low frequencies meaning it is a diffusion limited process. The semicircles diameters at high frequency region is closely correlative to the R_{ct}. As shown as the inset of Fig. 4B, a Randles model was chosen as the equivalent electrical circuit to fit all the data of EIS measurement. Here, R_s, R_{ct}, Z_w, CPE represented the solution resistance, the charge-transfer resistance of the redox probes, Warburg impedance and constant phase element, respectively. The simulated data of elements in equivalent circuit were shown in Table S2. The increased R_{ct} value of cDNA/GE (545 Ω, curve b) than that of GE (6.9 Ω, curve a)

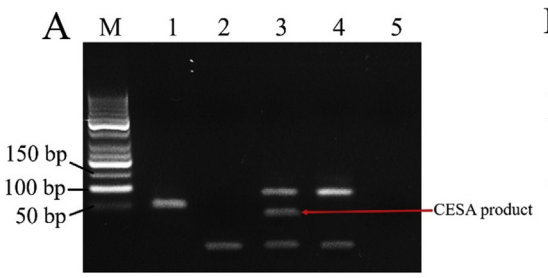

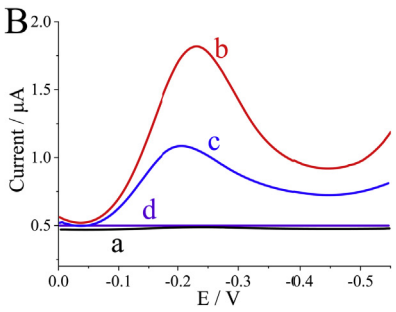

Fig. 3. Validation of DSA strategy for the detection of target miRNA. (A) Standard agarose gel electrophoresis of molecular events. Lane 1 to 5 referring to 1) cDNA, 2) miRNA, 3) cDNA + miRNA + DSN, 4) cDNA + miRNA, 5) no template control. Herein, agarose B low EEO, TAE buffer, 100 V, 30 min, 25 °C. (B) DPV dynamic curves of the cDNA/GE biosensors incubated with miRNA and detected with different methods. a) DSN and 3-QD@DNA NC with the blank sample (without miRNA), b) DSN and 3-QD@DNA NC with 100 aM miRNA, c) a QD@DNA NC with DSN incubated in 100 aM miRNA, d) 3-QD@DNA NC without DSN incubated in 100 aM miRNA. The electrolyte solution was 0.02 M Tris-HCl (pH 7.5, 25 °C). The electrolyte solution was 0.02 M Tris-HCl (pH 7.5, 25 °C). Scan rate: 100 mV/s.

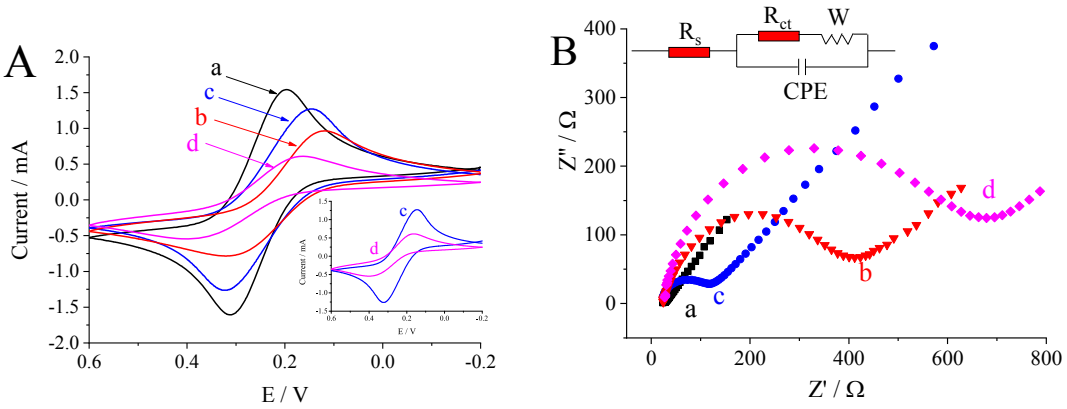

Fig. 4. (A) Cyclic voltammograms and (B) Nyquist plots of EIS for a) the bare GE, b) the cDNA/GE, c) the cDNA/GE + 100 aM miRNA + DSN, d) the cDNA/GE + CESA + 3-QD@DNA NC. The electrolyte solution of 5 mM $[Fe(CN)_6]^{3-/4-}$ and 0.5 M KCl. Scan rate: 100 mV/s.

indicated the formation of cDNA on the GE. When incubated with miRNA and DSN, the R_{ct} value of cDNA/GE decreased to 175 Ω (curve c), implying cDNA were cleaved on the GE by a target-triggered CESA. After incubated with 3-QD@DNA NC, the increased R_{ct} value of cDNA/GE (721 Ω, curve d) indicated that the hybridization of the cleaved cDNA with 3-QD@DNA NC blocked the electron transfer of the redox probes towards GE.

3.5. Optimal experimental conditions of the biosensor

Because both of DSN dosage and reaction time had critical influences on the properties of the biosensor, these factors were tested (Supporting Information, Figure S7), and 0.10 U DSN and 50 min reaction time were chosen as the optimal conditions.

Notably, the 3-QD@DNA NC on the cDNA/GE with a multiple-signal amplification (as shown as Fig. 3B), can be used as a direct electrochemical probe for the following detection of miRNA. The conditions, such as pH, buffer solutions, and hybridization time, had important effect on the sensitivity of the biosensor based on the 3-QD@DNA NC. All the experiments were tested (in Supporting Information, Fig. S8). And a Tris-HCl buffer solution (0.02 mol/L, pH 7.5) and 40 min was chosen as the optimal hybridization solution and time.

3.6. Application of this method for the detection of target miRNA

For quantitative detection of BRCA1 (a miRNA sequence screened from National Center for Biotechnology, Blast results in Supporting Information), different concentrations of miRNA sample (5 aM–5 fM) and the blank sample were incubated with the biosensor and detected. The DPV response of the biosensor were shown as Fig. 5A, and a linear relationship between the changes of current (ΔI) and the concentration of miRNA in range from 5 aM to 5 fM was recorded. The linear regression equation was ΔI (μA) = 0.391·lgC (aM) + 0.384 (r = 0.9956) (inset of Fig. 5A). Thus, a limit of detection (LOD) was 1.2 aM (DL = $3\delta_b$/K), which is two or three orders of magnitude lower than the LODs of 0.5 fM by Exo III exonuclease-based CESA (Cui et al., 2017) or 2.5 fM by SiO_2@Ag/DNA (You et al., 2018). Thus, this method with DSA strategy had superior performances for the detection of miRNA with a lower LOD (Table S3).

The selectivity of the biosensor was detected by DPV in the same concentration of target miRNA sample and other control samples, such as one-base (m1), three-base (m2) mismatch and non-complementary (m3) sequences. In Fig. 5B, compared with the target miRNA (100 aM), the mismatched and non-complementary sequences (10 fM) produced negligibly current responses, with a relative standard deviation (RSD) < 5%. This excellent selectivity might be ascribed to the specificity of the biosensor based on DSA strategy.

The stability of the biosensor was investigated by storing it a refrigerator (4 °C) for 30 days, and detected under the same condition. The decreased current responses were 2.0% for 5 days, 2.9% for 14 days and 4.8% for 30 days than the initial current response to 100 aM target miRNA, indicating its satisfactory stability. The intra-assay precision of this biosensor were tested by detecting 100 aM target miRNA for 5 replicate measurements with RSD of 0.8%, showing the satisfactory precision. Moreover, five batch-prepared biosensors also tested in the same condition, and the RSD of the inter-assay results was 2.5%, indicating a good reproducibility.

3.7. Real sample recovery tests

To investigate the application of target miRNA in real sample, the biosensor was employed to in healthy human serum sample. Recovery tests were performed using the standard addition method. And the analytical results were exhibited in Table S4. The recoveries ranged

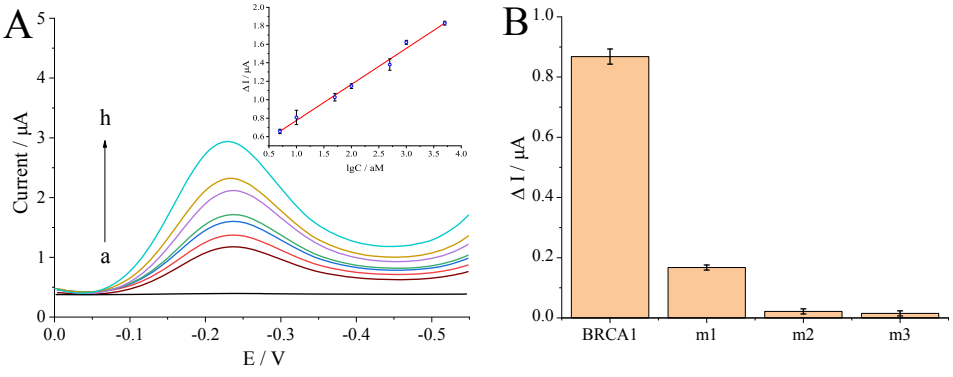

Fig. 5. (A) DPV responses of the DNA biosensor incubated with different concentrations of target miRNA. From a to i: 0, 5 aM, 10 aM, 50 aM, 100 aM, 500 aM, 1 fM, 5 fM, of BRCA1, inset: the calibration curve for the BRCA1 detection. (B) Selectivity of the DNA biosensor for the detection of BRCA1. The changes of current signal of 100 aM BRCA1, 10 fM m1 (one-base mismatch BRCA1 sequences), 10 fM m2 (three-base mismatch BRCA1 sequences), and 10 fM m3 (non-complementary sequence).

from 94.2% to 103% with RSD < 5%. Thus, the prepared DNA biosensor is desirable and qualified for practical sample determination.

4. Conclusion

In conclusion, an ultrasensitive DNA biosensor was developed for the detection of miRNA of BRCA1 by the DSA strategy, i.e. CESA and 3-QD@DNA NC. Compared with conventional biosensors, the method exhibited a better selectivity and sensitivity and had a detection limit of 1.2 aM of target miRNA in human serum samples. The improvement of analytical properties was ascribed to specificity of CESA and good amplification of both CESA and 3-QD@DNA NC. Furthermore, the method based on the DSA strategy is generic and can be used to detect low-abundance miRNA in clinical samples. Given its easy operation, high sensitivity, and high selectivity, this biosensor assay is potentially useful for clinical early diagnosis and treatment of breast cancer.

Author contribution statements

Song Zhang and Jilie Kong conceived of the presented idea. Bin Yang, Xueen Fang and Song Zhang carried out the experiment. Song Zhang and Jilie Kong supervised the project. All authors discussed the results and contributed to the final manuscript.

CRediT authorship contribution statement

Bin Yang: Data curation, Formal analysis, Investigation, Validation, Writing - original draft, Writing - review & editing. **Song Zhang:** Conceptualization, Data curation, Formal analysis, Funding acquisition, Investigation, Methodology, Project administration, Resources, Supervision, Validation, Visualization, Writing - original draft, Writing - review & editing. **Xueen Fang:** Data curation, Formal analysis, Investigation, Validation, Writing - original draft, Writing - review & editing. **Jilie Kong:** Conceptualization, Data curation, Formal analysis, Funding acquisition, Investigation, Methodology, Project administration, Resources, Supervision, Validation, Visualization, Writing - original draft, Writing - review & editing.

Acknowledgements

This work was supported by the National Natural Science Foundation of China (21505024, 21427806, 21175029, and 21335002), the Natural Science Foundation of Shanghai (19ZR1403300), the Introduce Talents of Fudan University Research Funding (JIH1615032) and the Shanghai Leading Academic Discipline Project (B109).

Appendix A. Supplementary data

Supplementary data to this article can be found online at https://doi.org/10.1016/j.bios.2019.111544.

Conflict of interest

The authors declare no competing financial interest.

References

Amin, R.M., Elfeky, S.A., Verwanger, T., Krammer, B., 2017. Biosens. Bioelectron. 98, 415–420.
Asaga, S., Kuo, C., Nguyen, T., Terpenning, M., Giuliano, A.E., Hoon, D.S.B., 2011. Clin. Chem. 57, 84–91.
Beenken, A., Mohammadi, M., 2009. Nat. Rev. Drug Discov. 8, 235.
Bo, B., Zhang, T., Jiang, Y., Cui, H., Miao, P., 2018. Anal. Chem. 90, 2395–2400.
Chan, M., Liaw, C.S., Ji, S.M., Tan, H.H., Wong, C.Y., Thike, A.A., Tan, P.H., Ho, G.H., Lee, A.S.G., 2013. Clin. Cancer Res. 19, 4477–4487.
Chen, J., Tang, L., Chu, X., Jiang, J., 2017. Analyst 142, 3048–3061.
Cui, M., Wang, Y., Wang, H., Wu, Y., Luo, X., 2017. Sens. Actuators B Chem. 244, 742–749.
Cuk, K., Zucknick, M., Heil, J., Madhavan, D., Schott, S., Turchinovich, A., et al., 2013. Int. J. Cancer 132, 1602–1612.
Duan, R., Zuo, X., Wang, S., Quan, X., Chen, D., Chen, Z., Jiang, L., Fan, C., Xia, F., 2013. J. Am. Chem. Soc. 135, 4604–4607.
Fan, T., Mao, Y., Sun, Q., Liu, F., Lin, J., Liu, Y., Cui, J., Jiang, Y., 2018. Cancer Sci. 109, 2897–2906.
Fish, L., Zhang, S., Johnny, X.Y., Culbertson, B., Zhou, A.Y., Goga, A., Goodarzi, H., 2018. Nat. Med. 24, 1743.
Jackson, S.P., Bartek, J., 2009. Nature 461, 1071.
Li, W., Ruan, K., 2009. Anal. Bioanal. Chem. 394, 1117–1124.
Li, C., Karadeniz, H., Canavar, E., Erdem, A., 2012. Electrochim. Acta 82, 137–142.
Li, W., Jiang, W., Ding, Y., Wang, L., 2015. Biosens. Bioeletron. 71, 401–406.
Liu, W., Li, L., Yang, S., Gao, J., Wang, R., 2017. Chem. Eur J. 23, 14177–14181.
Loo, A.H., Sofer, Z., Bouša, D., Ulbrich, P., Bonanni, A., Pumera, M., 2016. ACS Appl. Mater. Interfaces 8, 1951–1957.
Mavrogiannopoulou, E., Petrou, P.S., Kakabakos, S.E., Misiakos, K., 2009. Biosens. Bioelectron. 24, 1341–1347.
Mendell, J.T., 2016. N. Engl. J. Med. 374 (23), 2287–2289.
Michota, A., Bukowska, J., 2003. J. Raman Spectrosc. 34, 21–25.
Ng, E.K.O., Li, R., Shin, V.Y., Jin, H.C., Leung, C.P.H., Ma, E.S.K., et al., 2013. PLoS One 8, e53141.
Rasheed, P.A., Sandhyarani, N., 2015. Analyst 140, 2713–2718.
Rooij, E.V., Sutherland, L.B., Liu, N., Williams, A.H., McAnally, J., Gerard, R.D., Richardson, J.A., Olson, E.N., 2006. Proc. Natl. Acad. Sci. 103, 18255–18260.
Schrauder, M.G., Strick, R., Wendtland, R.S., Strissel, P.L., Laura, K., Loehberg, C.R., et al., 2012. PLoS One 7, e29770.
Seeman, N.C., 2003. DNA in a material world. Nature 421, 427.
Shi, L., Wang, Y., Chu, Z., Yin, Y., Jiang, D., Luo, J., et al., 2017a. J. Mater. Chem. B 5, 1073–1080.
Shi, L., Wang, Y., Ding, S., Chu, Z., Yin, Y., Jiang, D., et al., 2017b. Biosens. Bioelectron. 89, 871–879.
Shi, L., Rong, X., Wang, Y., Ding, S., Tang, W., 2018. Biosens. Bioelectron. 102, 41–48.
Siegel, R.L., Miller, K.D., Jemal, A., 2019. CA-Cancer. J. Clin. 69, 7–34.
Snell, C., Krypuy, M., Wong, E.M., Loughrey, M.B., Dobrovic, A., 2008. Breast Cancer Res. 10, R12.
Su, S., Fan, J., Xue, B., Yuwen, L., Liu, X., Pan, D., Fan, C., Wang, L., 2014. ACS Appl. Mater. Interfaces 6, 1152–1157.
Tavazoie, S.F., Alarcón, C., Oskarsson, T., Padua, D., Wang, Q., Bos, P.D., Gerald, W.L., Massagué, J., 2008. Nature 451, 147.
Umetani, N., Giuliano, A.E., Hiramatsu, S.H., Amersi, F., Nakagawa, T., Martino, S., Hoon, D.S., 2006. J. Clin. Oncol. 24, 4270–4276.
Vittala, S.K., Saraswathi, S.K., Joseph, J., 2017. Chem. Eur J. 23, 15759–15765.
Volinia, S., Galasso, M., Sana, M.E., Wise, T.F., Palatini, J., Huebner, K., Croce, C.M., 2012. Proc. Natl. Acad. Sci. U. S. A 109, 3024–3029.
Wang, Y., Bai, J., Qu, X., Gao, Y., Wang, J., Li, S., Fan, L., Wei, H., Liu, S., Peng, Y., 2018. Nanoscale 10, 18354–18361.
Wen, J., Zhou, S., Yu, Z., Chen, J., Yang, G., Tang, J., 2018. Biosens. Bioelectron. 100, 469–474.
Wilson, W.R., Hay, M.P., 2011. Nat. Rev. Cancer 11, 393.
Wu, Q., Lu, Z., Li, H., Lu, J., Guo, L., Ge, Q., 2011. J. Biomed. Biotechnol. 597145.
Xiao, K., Liu, J., Chen, H., Zhang, S., Kong, J., 2017. Biosens. Bioelectron. 91, 76–81.
Xu, H., Wang, L., Ye, H., Yu, L., Zhu, X., Lin, Z., Wu, G., Li, X., Liu, X., Chen, G., 2012. Chem. Commun. 48, 6390–6392.
Yang, H., Gao, Y., Wang, S., Qin, Y., Xu, L., Jin, D., Yang, F., Zhang, G.J., 2016. Biosens. Bioelectron. 80, 450–455.
Yin, B.C., Liu, Y.Q., Ye, B.C., 2012. J. Am. Chem. Soc. 134, 5064–5067.
You, M., Yang, S., Tang, W., Zhang, F., He, P., 2018. Biosens. Bioelectron. 112, 72–78.
Zhang, X., Xiao, K., Cheng, L., Chen, H., Liu, B., Zhang, S., Kong, J., 2014. Anal. Chem. 86, 5567–5572.
Zhang, X., Chen, B., He, M., Wang, H., Hu, B., 2016. Biosens. Bioelectron. 86, 736–740.
Zhao, Y., Hoshiyama, H., Shay, J.W., Wright, W.E., 2007. Nucleic Acids Res. 36, e14.
Zhao, W., Steinfeld, J.B., Liang, F., Chen, X., Maranon, D.G., Ma, C.J., Kwon, Y., Rao, T., Wang, W., Sheng, C., et al., 2017. Nature 550, 360–365.